UPPSALA
UNIVERSITET

UPTEC F16 019
Examensarbete 30 hp
Juni 2016

Estimation of Steering Wheel Angle in Heavy-Duty Trucks

Peter Fejes

UPPSALA
UNIVERSITET

Teknisk- naturvetenskaplig fakultet
UTH-enheten

Besöksadress:
Ångströmlaboratoriet
Lägerhyddsvägen 1
Hus 4, Plan 0

Postadress:
Box 536
751 21 Uppsala

Telefon:
018 – 471 30 03

Telefax:
018 – 471 30 00

Hemsida:
http://www.teknat.uu.se/student

Abstract

Estimation of Steering Wheel Angle in Heavy-Duty Trucks

Peter Fejes

The project presented in this report is a master's thesis performed at Scania CV. The main purpose is to develop an algorithm that estimates the offset of the values that the steering wheel angle sensor reports in a truck or tractor, and also to investigate the possibility to estimate the steering wheel angle in real-time. The developed algorithm successfully estimates the offset to an accuracy on the order of degrees, and the uncertainty of the estimate is ultimately determined by backlash in the steering system, which may range up to approximately 15 degrees or more depending on service standards. The investigation also shows that two general approaches to estimate the steering wheel angle in real-time can produce unbiased estimates only when the vehicle is cornering at low speeds.

Handledare: Mikael Johansson
Ämnesgranskare: Alexander Medvedev
Examinator: Tomas Nyberg
ISSN: 1401-5757, UPTEC F16 019

Populärvetenskaplig beskrivning

Inom produktutveckling är ett återkommande tema att höja en produkts värde genom att utnyttja dess komponenter på ett så smart sätt som möjligt. För produkter som innehåller datorliknande system, t.ex. allt från tvättmaskiner till flygplan, görs detta ofta genom att förändra dess mjukvara för att få exempelvis bättre funktionalitet eller säkerhet.

Det arbete som beskrivs i denna rapport handlar delvis om att skapa en funktion till lastbilar och dragbilar som automatiskt beräknar hur mycket en viss komponent, rattvinkelsensorn, är felaktigt inställd. Att upptäcka ett sådant fel är nödvändigt eftersom flera viktiga funktioner i fordonen, t.ex. antisladdsystem och styrning av bakhjul, är beroende av att rattvinkelsensorn fungerar korrekt. Dessutom krävs speciella verktyg och servicepersonal för att kalibrera en felinställd rattvinkelsensor. Metoden som tagits fram för att automatiskt upptäcka en sådan felinställning bygger på att utnyttja andra sensorer i fordonet, vilka kontinuerligt mäter hur snabbt dess hjul snurrar samt hur hela fordonskroppen roterar och accelererar. Detta flöde av mätdata används i ett datorprogram som körs på fordonets inbyggda datorsystem och då beräknar hur mycket rattvinkelsensorn är felinställd. En analys av den framtagna metoden visar att den kan uppskatta en eventuell felinställning till några graders noggrannhet. Vidare tyder analysen också på att noggrannheten av uppskattningen till stor del begränsas av små glapp i konstruktionen som sammankopplar ratt med framhjul.

Detta arbete behandlar också frågeställningen om den storhet som rattvinkelsensorn mäter möjligtvis kan beräknas helt utifrån mätdata från andra sensorer. Detta kan t.ex. vara användbart i en situation där en rattvinkelsensor plötsligt skulle sluta fungera. Eftersom lastbilar och dragbilar tillverkas i många olika variationer har en metod som är så generell som möjligt eftersökts. Slutsatsen av denna studie är att det är möjligt att skapa ett datorprogram till ett fordons inbyggda datorsystem som kontinuerligt uppskattar samma storhet som rattvinkelsensorn mäter. Noggrannheten hos de utvärderade metoderna beräknas vara i storleksordningen grader för ett fordon som svänger i låg fart, men vid höga farter uppträder ett systematiskt fel som beror på hur däck deformeras vid kurvtagning.

Acknowledgements

I would like to express my gratitude to everyone at Scania REVM and REVD for your welcoming and helpful attitudes. Writing this thesis with your support taught me valuable lessons in engineering and for that I will always be grateful. I would also like to dedicate special thanks to my mentor at Scania, Mikael Johansson, and also to professor Alexander Medvedev at Uppsala University.

Contents

1 Introduction **1**

1.1 Thesis objective 1

1.2 Report structure 1

2 Background **2**

2.1 The steering system 2

2.2 Ackermann steering geometry 3

2.3 Tire forces 4

2.4 Single-track vehicle models 5

2.4.1 Steady-state cornering equations 6

2.4.2 The handling diagram 7

2.4.3 Dynamic cornering equations 7

2.5 Sensor properties 9

3 Acquisition of validation data **12**

4 Real-time estimation **14**

4.1 Using steering geometry to estimate the SWA 14

4.2 Possibility to estimate SWA with the linear single-track model 18

4.3 Summary, conclusions, and further work 21

5 Offset estimation **23**

5.1 Description of the estimation algorithm 23

5.1.1 Signal pre-processing 24

5.1.2 Evaluation of the vehicle's motion 26

5.1.3 Computation of SWA offset 27

5.2 Statistical foundation of the estimation principle 28

5.3 Theoretical performance 30

5.3.1 Errors related to the yaw rate sensor 31

5.3.2 Errors related to the accelerometer 31
5.3.3 Errors related to backlash in the steering system 32
5.4 Results 33
5.5 Discussion 35
5.5.1 Possible further processing of the SWA estimate 35
5.5.2 Efficacy of the motion filter 36
5.5.3 The accelerometer signal 36
5.5.4 Using other sensors for the estimation 37
5.6 Summary, conclusions, and further work 37

Nomenclature

Acronym	Description
CAN	Controller Area Network
OLS	Ordinary Least Squares
RLS	Recursive Least Squares
SWA	Steering Wheel Angle
SAS	Steering Wheel Angle Sensor
YRS	Yaw Rate Sensor

Symbol	Description	Unit
r	Yaw rate	rad/s
v_x	Longitudinal speed	m/s
v_y	Lateral speed	m/s
a_y	Lateral acceleration	m/s
δ	Steering wheel angle	rad
δ_o	Steering wheel angle offset	rad
δ_f	Steering angle	rad
α_f	Mean tire slip angle of front axle tires	rad
α_r	Mean tire slip angle of rear axle tires	rad
β	Vehicle side-slip angle	rad
C_f	Cornering stiffness of front tires	N/rad
C_r	Cornering stiffness of rear tires	N/rad
I_z	Vehicle moment of inertia about its center of gravity and vertical axis	kg m^2
m	Vehicle mass	kg
l_f	Distance from front axle to vehicle center of gravity	m
l_r	Distance from rear axle to vehicle center of gravity	m
L	Wheel base	m
L_e	Equivalent wheel base	m
R	Turn radius	m
i_{gear}	Overall steering gear ratio	1

1 Introduction

Numerous vehicles that Scania CV delivers are equipped with a steering wheel angle sensor (SAS). Apart from its key role in the Electronic Stability Program system that is now mandatory for most new heavy vehicles in the European Union, this sensor is important to functions related to, for example, electric power steering, steering of rear axes, adaptive cruise control, and intelligent forward lighting.

The installed SAS measures the absolute angle of the steering wheel, and today calibration is performed in the production process and also at service workshops when needed. If, however, this calibration is not done after mechanical adjustments of the steering system or after installing a new SAS, an offset might enter the signal. This, in turn, might cause unwanted effects in the functions relying on steering wheel angle (SWA) information, and for this reason it is of interest to automatically detect and compensate for possible offset errors.

1.1 Thesis objective

The objective of the work presented is

1. to investigate the possibility to use the measurements from commonly installed sensors to estimate the SWA in real-time and
2. to develop an algorithm that estimates the offset in the values reported by the SAS.

1.2 Report structure

This report is structured into the four main sections background, data acquisition, real-time estimation, and offset estimation.

The background, covered in chapter 2, gives an introduction to the construction of the steering system, sensor properties, and also the relevant theory of vehicle dynamics. In the chapter about data acquisition it is explained what equipment was used and how the test to gather validation data was performed. Chapter 3 contains the investigation on the possibility to estimate the SWA in real-time, and lastly chapter 4 covers the entire topic on the developed algorithm for estimating the SWA offset.

2 Background

2.1 The steering system

The steering system consists of the components that give the driver directional control of the vehicle. While some vehicle configurations have multiple steered axes, the components relevant to this thesis are those that steer the front wheels.

Fig. 1 illustrates the structure of a typical heavy-duty truck steering system where the steering wheel inputs torque to the steering gear, which turns the front wheels via linkages as shown.

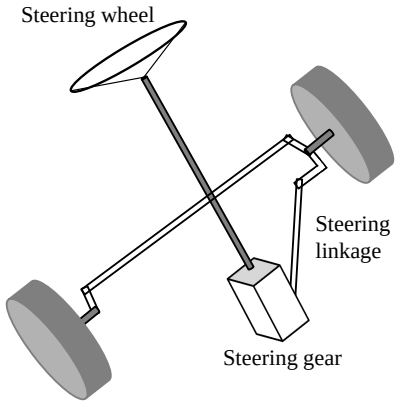

Figure 1: Schematic view of a truck steering system

The ratio between input angle to output angle of the steering gear can be fixed or variable and is usually around 20:1. Also, the steering gear is hydraulically assisted, meaning that it will have a certain characteristic between the input and output torque.

Because the steering system consists of gears and several joints there may be some backlash seen between the steering wheel angle and the angle of the front wheels. A maintenance standard for heavy trucks found in literature is that a maximally acceptable backlash between steering wheel and front wheels is 15 ° [1] in the meaning that the steering wheel is allowed to be turned maximally 15 ° before turning of the front wheels is observed.

Also, regarding small adjustments of the steering wheel around the steering center,

i.e. around 0 ° SWA, it is generally pursued that the vehicle should stay on its trajectory. If not, the driver will constantly have to input steering corrections for even the smallest disturbances from road irregularities or wind [2].

The steering system also plays an important role to the handling characteristics of the vehicle where one design parameter is the torsional stiffness seen between the steering wheel angle and the front wheel angles. In other words, the steering system is designed to be flexible in a certain way.

The SAS is mounted to the shaft just below the steering wheel and therefore both flexing and backlash of/in the steering system may have to be accounted for when trying to convert the angles of the front wheels to SWA or vice versa.

2.2 Ackermann steering geometry

During cornering all wheels travel at different speeds. To allow each wheel to roll freely, steering systems are designed to resemble Ackermann steering geometry. This geometry is achieved when the heading of each wheel is perpendicular to the same turning center as shown in Fig. 2.

However, in practice the arrangement of the linkages that turns the wheels result in perfect Ackermann steering geometry at only one turning angle. In general, for heavy-duty trucks the deviation from Ackermann steering geometry has to be the smallest at low turning angles and at high longitudinal speeds [1]. Also, at near-maximum turning angles it is not uncommon that the actual steering geometry differs more from the ideal one.

By assuming Ackermann steering geometry the relation

$$\frac{v_r}{R_r} = \frac{v_l}{R_l} \tag{1}$$

can be formulated, where v_r and v_l are the velocities of the right and left front wheel, respectively, and R_r and R_l are the corresponding turn radii as shown in Fig. 2.

From the geometric relations of Fig. 2 the mean front wheel steer angle can then be written as

$$\delta_f = \frac{1}{2} \arcsin\left(\frac{2L}{L_{tw}} \frac{\frac{v_l^2}{v_r^2} - 1}{\frac{v_l^2}{v_r^2} + 1 - \frac{L_{tw}^2}{2R_l^2}} \right) \tag{2}$$

and since $\frac{L_{tw}^2}{2R_l^2} \ll 1$ and $\frac{v_l}{v_r} \approx 1$ this equation can be simplified and approximated into

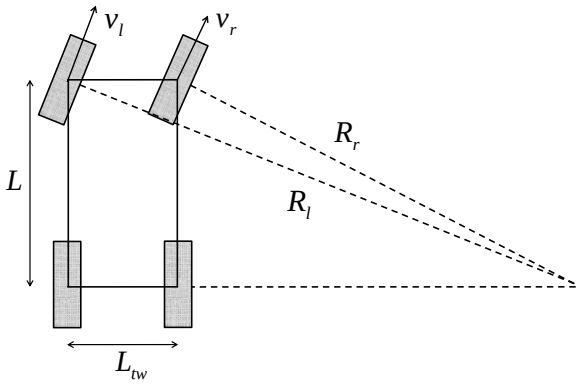

Figure 2: Ackermann geometry

the computationally more suitable form

$$\delta_f = \frac{1}{2} \arcsin\left(\frac{4L}{L_{tw}} \frac{v_l - v_r}{v_l + v_r}\right). \tag{3}$$

2.3 Tire forces

Extensive research has been done on the interaction between vehicle tires and road, resulting in models with a wide range of complexity. The most basic, yet widely used, model relates the force generated perpendicular to the plane of the wheel as

$$F_y = C\alpha \tag{4}$$

where C is a constant called cornering stiffness and α is the slip angle, defined as the angle between the heading and the velocity of the tire as illustrated in Fig. 4. This linearisation is considered valid for slip angles less than $5\,^\circ$ and when the vertical load on the tire remains constant[3]. Regarding the slip angles of the tires of a heavy truck, these rarely exceed $2\,^\circ$ during normal driving and therefore stay in the linear range [4].

The value of C is essentially directly proportional to the vertical load on the tire and is for truck tires about 8%-10% and 11%-19% of the vertical force on bias-ply and radial-ply tires, respectively [5].

When a tire is turned, the change in lateral force it produces is not immediate. This transient can be described by the first-order differential equation

$$\tau \frac{d}{dt}\tilde{F_y} + \tilde{F_y} = F_y \tag{5}$$

where F_y is the steady-state value of the lateral force [6]. The magnitude of the time-constant τ is related to the distance the tire has to roll for the deformation of the contact-patch to reach a steady-state shape. Writing the time-constant as

$$\tau = \frac{\sigma_r}{v_x} \tag{6}$$

where v_x is the vehicle's longitudinal speed, this distance, σ_r, will be on the same order as the wheel radii when the vertical load on the tire is nominal [7].

The point where the resultant lateral force acts at a tire is generally behind the geometric center of the contact patch between the tire and road. This, together with the inclination of the kingpin creates a moment, M_{SAT}, as illustrated in Fig. 3. This moment has a direction such that it acts to restore the tire to its neutral position and is therefore called self-aligning torque.

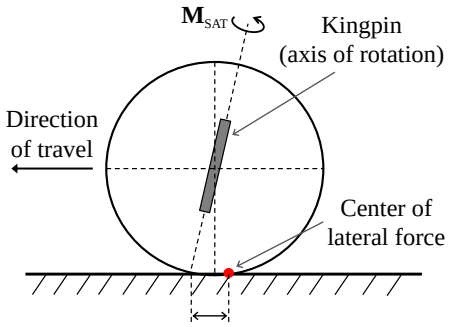

Figure 3: Side view of a tire developing self-aligning torque.

2.4 Single-track vehicle models

The single-track model is commonly used in the analysis of a road vehicle's dynamics. The basic idea of the model is that it lumps each pair of left and right wheels into one wheel. This greatly simplifies the otherwise complicated problem and is useful for studying lateral and longitudinal vehicle motion.

In the following sections the only forces acting on the modeled vehicle are the ones originating from the contact between tires and road. Aerodynamic forces such as drag or cross-wind are neglected.

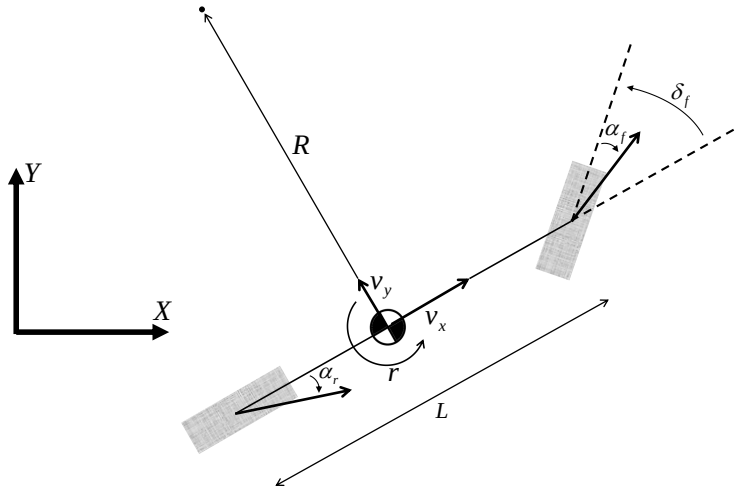

Figure 4: Single-track model of a vehicle. The symbols α_f and α_r represent the angle between the heading and velocity of the front and rear wheels, respectively.

2.4.1 Steady-state cornering equations

A single-track model of the simplest wheel axle configuration, i.e. one front axle and one rear axle, is shown in Fig. 4. Here, δ_f denotes the steering angle, α_f and α_r the front and rear tire slip angles, R the turn radius, and v_x and v_y the vehicle's longitudinal and lateral speed in the vehicle-fixed coordinate system. The yaw rate, r, is the rate of rotation measured with respect to the earth-fixed coordinate axis X.

A vehicle can be said to be cornering at a steady state when the quantities turn radius, longitudinal speed, and tire slip angles all are constant. In the case of a low longitudinal speed, e.g. less than 5 m/s, and when the turn radius is much larger than the wheelbase the steering angle can be approximated as [3]

$$\delta_f = \frac{L}{R} \tag{7}$$

with notations according to Fig. 4. This angle is called the Ackermann steering angle. For real, two-axle vehicles the magnitude of the wheelbase generally needs to be slightly adjusted to fit (7) [8].

At higher vehicle speeds the slip angles of the tires have to be taken into account and

then the steady-state cornering solution becomes [3]

$$\delta_f = \frac{L}{R} + \alpha_f - \alpha_r. \tag{8}$$

which generally can be written as

$$\delta_f = \frac{L}{R} + f(a_y), \tag{9}$$

meaning that the difference between front and rear tire slip angles is a function of the lateral acceleration. With the assumption of linear tire properties as described in section 2.3, (8) can be written on the form

$$\delta_f = \frac{L}{R} + \frac{K_{us}}{g} a_y \tag{10}$$

where g is the gravitational constant and K_{us} is a constant called the understeer gradient [3].

The steady-state equations for single-track models of vehicles with multiple, non-steered rear axles and/or dual tires can be expressed as

$$\delta_f = \frac{L}{R} + f_1(a_y, v_x) \tag{11}$$

or alternatively

$$\delta_f = \frac{L}{R} + f_2(a_y, 1/R). \tag{12}$$

C.B. Winkler [8] showed that the the functions f_1 and f_2 in equations 11 and 12 decrease their dependence of v_x and $1/R$, respectively, if the wheelbase, L, is substituted with an equivalent wheelbase, L_e.

2.4.2 The handling diagram

In 1973 H.B. Pacejka introduced the handling diagram as an aid to his analysis of the steady-state turning behavior of a single-track vehicle model. In one of its forms, this diagram displays the quantities $\frac{L}{R}$ and $\alpha_r - \alpha_f$ from (8) as functions of lateral acceleration as shown in Fig. 5. As the steering angle equals to the horizontal distance between two corresponding curves, this approach makes it easy to apprehend the relationship between steering angle, velocity, and lateral acceleration.

2.4.3 Dynamic cornering equations

The dynamic, linear single-track equation of motion is often written as

$$\begin{bmatrix} \dot{r} \\ \dot{\beta} \end{bmatrix} = \begin{bmatrix} -\frac{1}{v_x}\frac{2(C_f l_f^2 + C_r l_r^2)}{I_z} & -\frac{2(C_f l_f - C_r l_r)}{I_z} \\ -1 - \frac{1}{v_x^2}\frac{2(C_f l_f - C_r l_r)}{m} & -\frac{1}{v_x}\frac{2(C_f + C_r)}{m} \end{bmatrix} \begin{bmatrix} r \\ \beta \end{bmatrix} + \begin{bmatrix} \frac{2C_f l_f}{I_z} \\ \frac{1}{v_x}\frac{2C_f}{m} \end{bmatrix} \delta_f \tag{13}$$

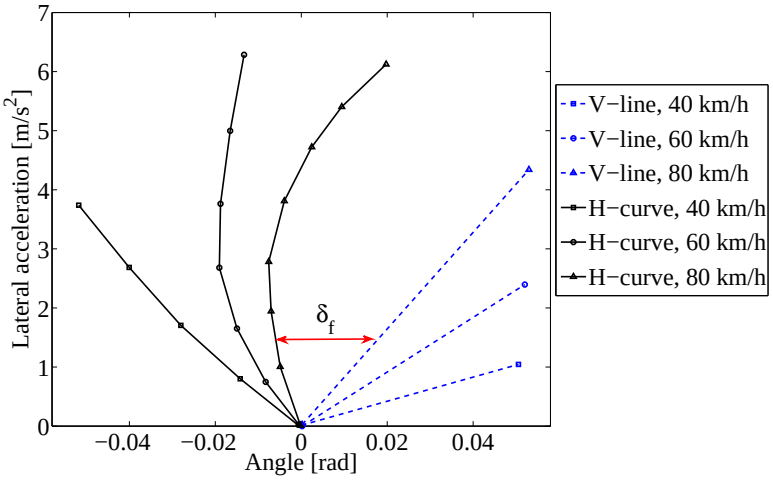

Figure 5: Example of a handling diagram for a nonlinear vehicle. 'V-line' and 'H-curve' denotes the quantities $\frac{L}{R}$ and $\alpha_r - \alpha_f$, respectively. For illustrative purposes the differences between the H-curves are exaggerated, meaning that real vehicles generally have H-curves located more closely to each other.

with notations according to Fig. 6. As earlier, r is the yaw rate of the vehicle, l_f and l_r distances from front and rear axle to the vehicle center of gravity, and I_z and m are the vehicle's moment of inertia and mass, respectively. The longitudinal speed, v_x, is treated as a constant and the state variable β is the vehicle side-slip angle defined as

$$\beta = \tan^{-1}\left(\frac{v_y}{v_x}\right). \tag{14}$$

(13) is derived by first applying Newton's second law of motion as

$$\begin{cases} ma = mv_x(\dot{\beta} + r) = 2F_f + 2F_r \\ I_z\dot{r} = 2l_fF_f - 2l_rF_r \end{cases} \tag{15}$$

and then using small-angle approximations while substituting the terms F_f and F_r by using the kinematic relations

$$\alpha_f = \frac{v_y + l_f r}{v_x} - \delta_f \tag{16}$$

and

$$\alpha_r = \frac{v_y - l_r r}{v_x} \tag{17}$$

together with the tire force model

$$F_i = -C_i\alpha_i \quad i = f, r. \tag{18}$$

The steady-state solution to (13) is (10).

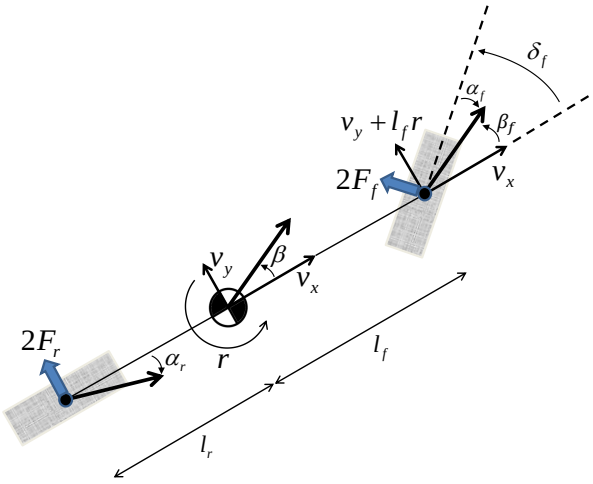

Figure 6: Scheme of the commonly used single-track model.

2.5 Sensor properties

This section covers the important aspects of the sensors used in this thesis. These are standard sensors in vehicles equipped with ESP, and the quantities of interest that are broadcast on the Controller Area Network (CAN) in these vehicles are

- yaw rate,
- lateral/longitudinal acceleration,
- steering wheel angle,
- vehicle speed, and
- wheel speeds.

The sensors supplying measurements for this information are of typical automotive grade with specifications of some listed in Tab. 1. Worth noting is that the listed values of resolution may be higher depending on the CAN set-up. In addition to the properties listed in Tab. 1, automotive grade SAS typically have a maximum tolerated hysteresis span of 5 ° over the full measuring range.

The accelerometer and gyroscope are Micro-Electro-Mechanical Systems (MEMS) type sensors. Due to the design of these, a technical parameter called 'bias drift' is critical paying attention to. Even in the absence of input to a MEMS gyroscope/accelerometer,

Sensor	Resolution	Range	Offset
SAS	$0.1\,^\circ$	$1500\,^\circ$	$< 2.5\,^\circ$ (from hysteresis)
Yaw rate sensor	$0.1\,^\circ/s$	$100\,^\circ/s$	$< 3\,^\circ/s$
Accelerometer	0.01 g	2 g	< 0.1 g

Table 1: Specifications for typical automotive grade sensors.

i.e. subjecting the device to rotation/acceleration, the output will vary as time goes. This bias drift, measured in $^\circ/s/min$ or $m/s^2/min$, has complex, nonlinear behaviors due a combination of time, temperature and acceleration [9]. There are usually mechanisms to compensate the drift on sensor level, though it is not completely mitigated. During the first 15 minutes of operation, it is not uncommon to observe bias-drifts of up to $1.0\,^\circ/s/min$ of a MEMS gyroscope and up to 0.03 g/min of a MEMS accelerometer.

Finally, the wheel and vehicle speed information is obtained with adaptive sensor fusion techniques and is based on tachometer readings of the angular rates at the wheels and the transmission output shaft.

Effect of the road's horizontal slope

It is common practice to construct roads to be slightly horizontally angled for drainage of surface water. Also, when needed at a curved road section an additional angle is added to counteract the otherwise large centrifugal force acting on a turning vehicle.

For highways and arterial roads in many countries, the design policy for horizontal slope is typically about 2 % (equivalent to $1.1\,^\circ$) and recommended maximum slope of curved sections is typically around 7-8 % (equivalent to $4.0\,^\circ$-$4.6\,^\circ$) [10].

If neglecting the additional chassis roll angle that results from the suspension and tires experiencing a shifted center of gravity, a sensor measuring acceleration along a vehicle's longitudinal axis will measure the component of the gravitational acceleration

$$a_{y,g} = g\, sin(\theta_{bank}) \tag{19}$$

with symbols as defined in Fig. 7.

In the case where a vehicle travels straight-ahead on a horizontally angled road with negligible centrifugal forces acting on it, the measured lateral acceleration according to (19) will be about 0.2 m/s^2 at 2 % and 0.7 m/s^2 at 7 % horizontal slope.

The measuring principle of MEMS gyroscopes typically makes them unaffected by

bank angle. Specifications of automotive grade gyroscopes allow for shifts in yaw rate of about 0.1 mrad/s to 0.3 mrad/s at 2 % to 7 % horizontal slope.

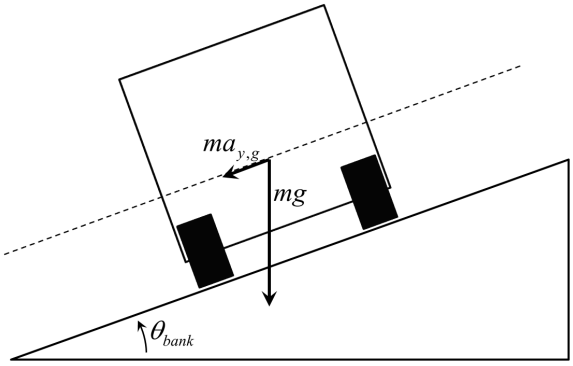

Figure 7: Illustration of a vehicle traveling on a horizontally angled road.

3 Acquisition of validation data

To evaluate the performance of the developed offset estimation algorithm, validation data were collected by logging accurate GPS measurements and also the signals of interest on the CAN while driving a 4x2 tractor.

Relevant specifications of the tractor are listed in Tab. 2 and the GPS receiver used was an Oxford RT3040, which is a highly accurate measurement device that combines GPS signals with measurements from a 3-axis accelerometer and a 3-axis gyroscope. The resolution in heading is specified to be 0.1° to one standard deviation.

To begin with, the tractor was driven around the track illustrated in Fig. 8 for about 30 minutes at speeds between 20 to 90 km/h and with a mean speed of 50 km/h.

Figure 8: Map of the path where the tractor was driven.

After driving around the track the tractor was driven back and forth on an outlined, straight road section to estimate the SWA offset. The longitudinal speed was kept in the range 10.0-10.5 km/h and the geographical position measurements from the Oxford RT3040 had an estimated standard deviation of 0.5 m at a measurement frequency of 100 Hz.

Fig. 9 shows the measurement results where the mean SWA when going back and forth over the same, straight road section is 2.04° with a standard deviation of 1.19°.

Model	R730 LA4x2MNA
Wheelbase	3.700 m
Steering gear	ZF Servotwin
Steering gear ratio (near center)	19.3
Wheel configuration	4x2
Chassis type	Tractor

Table 2: Specification of the truck used.

The upper SWA trend has a mean of 3.60 ° and the lower SWA trend's mean is 0.48 °

By going both ways along the same geographical path the influence on SWA from the road's horizontal slope is minimised. As seen in the lower graph of Fig. 9 the measured lateral acceleration, which is directly affected by road bank angle, is mirrored.

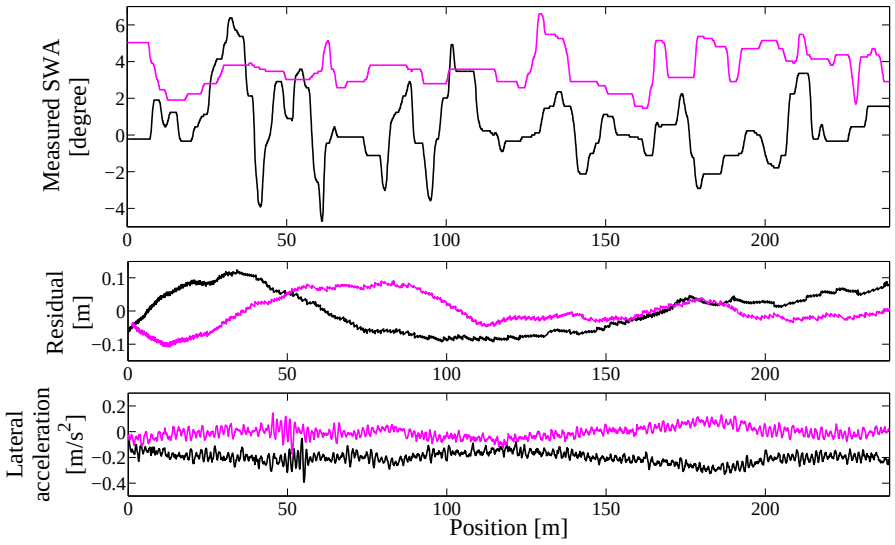

Figure 9: Logged sensor readings while driving in both directions over the same geographical path. The purple lines represent driving in one of the directions and the black lines represent driving the opposite. The residual is calculated as the deviation from the best fit of the GPS data to a straight line.

4 Real-time estimation

At the time when this thesis was carried out, searches on the topic of estimating the SWA in databases of e.g. Society of Automotive Engineers, academic publications, and among patents resulted in no matches with the exceptions of a few patents that use the principle of Ackermann geometry to estimate the mean front wheel angle.

The available sensors measure motion of the wheels and the vehicle's body, and because of this the strategy for estimating the SWA will be to first estimate the mean angle of the front wheels and from this angle compute the SWA.

Since a model that relates front wheel angle to SWA is specific to the vehicle, e.g. depends on what steering gear and linkages that are installed, the focus of this chapter will be to estimate the mean front wheel angle. Conversion to SWA will then be a matter of using an approximation of one of Scania's more detailed models of the steering system.

A challenge in using a detailed model of the steering system, however, is that the steering torque, which is central in such a model, normally is not measured and thus would need to be estimated.

In the following, the possibilities of estimating the front wheel angle using two different approaches will be laid out. The first approach is based on the wheel speed sensors and geometry of the steering system while the second approach builds on the linear single-track model and measurements of the vehicle's inertial motion.

4.1 Using steering geometry to estimate the SWA

To estimate the front wheel angle using (3) the individual speeds of the left and right front wheels have to be calculated. The natural choice for this calculation is to use the wheel angular speed sensors and the relation

$$v_i = r_i \omega_i \tag{20}$$

where r_i is the wheel radius and ω its rotational speed. Combining (20) with (3) results in

$$\delta_f = \frac{1}{2} \arcsin\left(\frac{4L}{L_{tw}} \frac{\omega_l \frac{r_l}{r_r} - \omega_r}{\omega_l \frac{r_l}{r_r} + \omega_r} \right) \tag{21}$$

where it is seen that the term r_l/r_r has entered. For improved accuracy, this term can for example be estimated using a method by Gustafsson et al., which is explained further in section 5.3.1.

The reason for using the signals from the front wheels is because (20) means that the wheel is rolling perfectly, i.e. does not slide, and generally the front wheels of heavy-duty trucks are not driven by the motor.

Properties of the estimation principle

Some properties of (21) are demonstrated in figures 10, 11, and 12. In the simulations corresponding to figures 10 and 11 data from the test described in chapter 3 were used. The data used to produce Fig. 12 originate from another test with a vehicle of similar specifications. Conversion between front wheel angle to SWA is performed with a 4^{th} order polynomial approximation of the steering system's gear ratio.

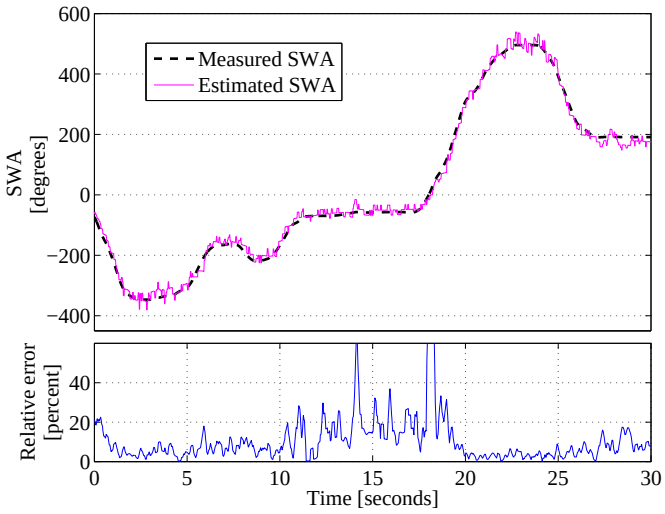

Figure 10: Estimated SWA when cornering at a mean speed of 17 km/h.

To begin the analysis, a low speed manoeuvre as shown in Fig. 10 is considered. The mean speed during this manoeuvre is 17 km/h and it is seen that the relative error generally stays below 10 % for SWAs larger than about 200 ° and oscillates around 20 % for SWA smaller than 200 °.

Next, a manoeuvre at a mean speed of 46 km/h is considered in Fig. 11 . Again, a relative estimation error of about 20 % is seen. Also, the SWA appears to be underestimated at the largest amplitudes around the 5-10 and 20 second mark, where the SWA is underestimated by around 20 ° and 15 ° respectively.

To get a sense of the errors that arise during transient motion, (21) is tested on data

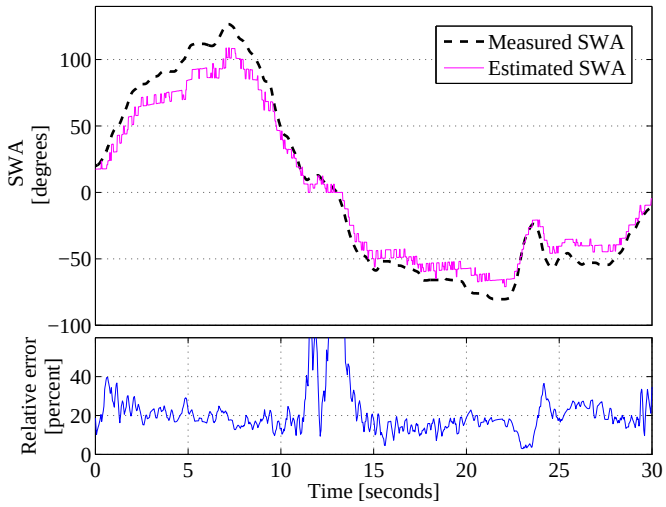

Figure 11: Estimated SWA when cornering at a mean speed of 46 km/h.

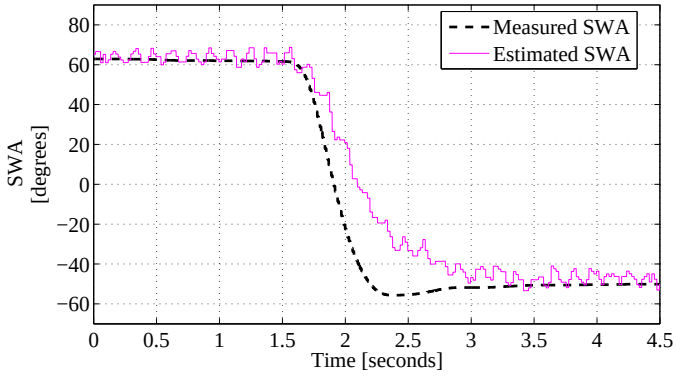

Figure 12: Estimated SWA during a hard turn at 72 km/h.

from an experiment where the steering wheel was connected to and controlled by an electric motor. As seen in Fig. 12 the SWA was programmed to change from about 60 ° to -50 ° and did so at a rate of nearly 260 °/s. The time for the estimated value to reach 90 % of the change, i.e. go from 60 ° to -29 °, is 0.85 seconds.

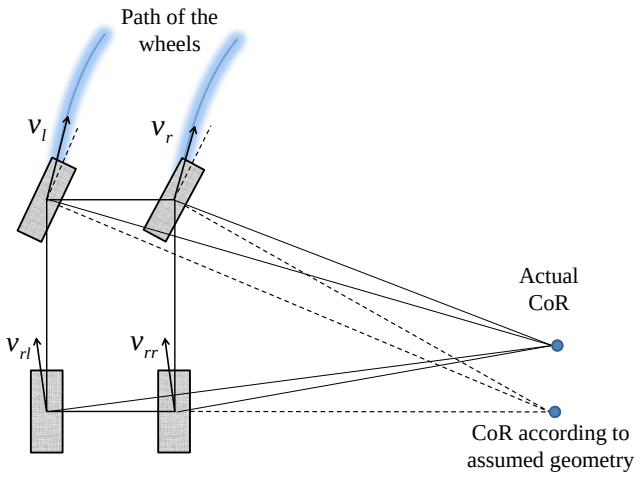

Figure 13: Illustration of why the estimation method gives a too small estimate during cornering when the tires develop significant slip angles.

Discussion and conclusions

As seen in Fig. 10, the estimate appears to be unbiased in the SWA range of -500 ° to 500 °. However, at larger angles than these the actual geometry of the steering system often deviates from Ackermann steering geometry, and thus an estimate that is intended to produce accurate estimates over the full SWA range would require additional corrections for this deviation.

The behavior seen in Fig. 11 where the SWA is underestimated can be explained by the fact that the tires are developing significant slip angles because the turn is performed at a higher speed. This effect is illustrated in Fig. 13 where it is shown how the actual center of rotation (CoR), the instantaneous point at which the vehicle's motion rotates about, is no longer aligned with the rear axis as is assumed by Ackermann theory. Deriving a general compensation for this error is non-trivial because a tire that exhibits a slip angle is deformed and some slip occurs at the area that is in contact with the road, meaning that (20), which is fundamental to this SWA estimate, may no longer hold.

If, however, the quantity $\frac{\omega_l r_l}{\omega_r r_r}$ remains unchanged despite non-zero slip angles, (21) will produce an estimated front wheel angle that is nearly equivalent to the Ackermann steering angle, $\frac{L}{R}$, given that the slip angles of the rear axle tires are low, e.g. below 2 °. This assumption seems to hold as is shown in Fig. 14, where this SWA estimate is compared to an estimate of the Ackermann steering angle computed from the yaw rate

sensor. Then, by considering the equation

$$\delta_f = \frac{L}{R} + \alpha_f - \alpha_r \approx \frac{L}{R} + \frac{K_{us}}{g} a_y \tag{22}$$

that is presented in section 2.4.1 it is seen how a better estimate can be obtained by adding correction corresponding to the quantity $\alpha_f - \alpha_r \approx \frac{K_{us}}{g} a_y$. However, as is explained in section 4.2 it is not possible to estimate either α_f or K_{us} without the use of a SAS. Because K_{us} depends on the vehicle's mass and how it is distributed, further investigation will have to show whether K_{us} can be supplied as a parameter specific to the vehicle configuration in order to improve accuracy of a SWA estimate. Also, if trying to implement such a correction, special care must be taken when the brakes are applied in a curve. In this situation the cornering force is generally reduced as compared to a situation with pure side-slip [5].

Finally, Fig. 12 is presented to demonstrate the important fact that (21) fundamentally estimates the SWA during cornering at a steady-state. Taking into consideration the large moment of inertia of a truck, the compliance of the steering system, and also the time transient of produced lateral force at the tires, it is obvious that the vehicle's motion lags a change in the SWA. If only measurements of the vehicle's motion are to be used to estimate the SWA, the ideal method for this will therefore involve predictive models.

4.2 Possibility to estimate SWA with the linear single-track model

Until now, only the rotational speed of the wheels has been considered in an attempt to estimate the SWA. As mentioned earlier, there are available measurements of the vehicle's motion from an accelerometer and a gyroscope. By also including GPS measurements additional valuable quantities can be obtained. In the following it will be investigated if measurements from these sensors can be used together with the linear single-track model to estimate the front wheel angle.

The gyroscope provides the yaw rate directly and the accelerometer the lateral acceleration. However, the common approach to obtain the vehicle side-slip angle, β, is to estimate it by using a set of sensors that includes the SAS [11]. It has been shown that a single-antenna, consumer-grade GPS receiver in combination with a yaw gyroscope is sufficient to estimate the vehicle side-slip angle and to even better accuracy when using a dual-antenna GPS system [12]. To take the argument of whether it is possible to estimate the SWA further it is from here on assumed that the vehicle side-slip angle is not obtained by using the SAS and instead e.g. obtained by using GPS measurements.

Now, considering the single-track model in Fig. 6 it is seen that the way the front wheel angle δ_f is related to the motion of the vehicle's body is through the angle of the speed vector at the front wheel, β_f, as

$$\delta_f = \beta_f - \alpha_f. \tag{23}$$

A simple kinematic relation gives the angle β_f as

$$\beta_f = \tan^{-1}\left(\frac{v_y + ar}{v_x}\right) \tag{24}$$

where a is the distance between the front axle and the point at which the vehicle side-slip angle is measured. This means that the critical part in estimating the front wheel angle with this approach is to obtain α_f.

The foundation of the linear single-track model is the geometric set-up as seen in Fig. 6, Newton's second law of motion, and a simple linear model for lateral force at the tires, $F_y = C\alpha$. This gives the system of equations

$$\begin{cases} -C_f\alpha_f - C_r\alpha_r = \frac{m}{2}v_x(\dot{\beta} + r) \\ -l_f C_f\alpha_f + l_r C_r\alpha_r = \frac{I_z}{2}\dot{r} \end{cases} \tag{25}$$

and because both C_f and α_f are unknown and only occur in the multiplied term $C_f\alpha_f$ it is not possible to solve for α_f alone, which in turn makes it impossible to obtain δ_f.

This can also be seen from the full set of equations

$$\begin{cases} C_f\delta_f - C_f x_1 - C_r x_2 = \frac{m}{2}x_3 \\ l_f C_f\delta_f - l_f C_f x_1 + l_r C_r x_2 = \frac{I_z}{2}x_4 \end{cases} \tag{26}$$

where for ease of reading the quantities that directly or indirectly can be obtained from sensor measurements are denoted as

$$\begin{cases} x_1 = \beta_f \\ x_2 = \alpha_r \\ x_3 = v_x(\dot{\beta} + r) \\ x_4 = \dot{r}. \end{cases} \tag{27}$$

The system 26 clearly has more unknowns than equations considering that the cornering stiffness parameters, C_f and C_r, largely depend on what kind of tires that are used, how many tires that are mounted per axle, the vertical load on the axle, inflation pressure etc. This leads to the conclusion that it is not possible to directly solve the linear single-track model for the front wheel angle δ_f.

With regression methods an underdetermined system of equations can sometimes be solved by supplying a number of independent measurements such that a new, solvable system of equations can be formulated. If it were possible to first estimate the constants l_f, l_r, C_f, C_r, m, and I_z or a suitable combination of these it would then be possible to estimate the front wheel angle from the equations of 26. The general idea is in other words to first estimate these unknown constants by a regression method, e.g. linear regression by the least mean squares method, and then insert the estimated values into equations 26 and compute an estimate of the front wheel angle, δ_f, in real-time.

The main problem in applying such an approach lies in formulating the equations of the linear single-track model into an expression that is suitable for regression analysis. Rewriting the equations 26 into matrix form as

$$\begin{bmatrix} C_f & -C_f & -C_r & -\frac{m}{2} & 0 \\ C_f & -C_f & \frac{l_r}{l_f}C_r & 0 & -\frac{I_z}{2l_f} \end{bmatrix} \begin{bmatrix} \delta_f \\ x_1 \\ x_2 \\ x_3 \\ x_4 \end{bmatrix} = \begin{bmatrix} 0 \\ 0 \end{bmatrix} \tag{28}$$

and then multiplying the upper equation with a factor λ followed by addition of the two equations yields the expression

$$\begin{bmatrix} (\lambda+1)C_f & -(\lambda+1)C_f & (\frac{l_r}{l_f}-\lambda)C_r & -\lambda\frac{m}{2} & -\frac{I_z}{2l_f} \end{bmatrix} \begin{bmatrix} \delta_f \\ x_1 \\ x_2 \\ x_3 \\ x_4 \end{bmatrix} = 0 \tag{29}$$

from which it can be seen what possible expressions there are to work with by adjusting the value of λ. It is now seen that eliminating δ_f, i.e. choosing $\lambda = -1$, is not suitable as this would also eliminate C_f. This fact that δ_f cannot be eliminated implies that a converging solution for the constants in the linear single-track model cannot be guaranteed as long as δ_f is time-varying.

When the front wheel angle, δ_f, is constant and non-zero the vehicle is cornering at steady-state. At such conditions (29) reduces into

$$\begin{bmatrix} (\lambda+1)C_f & -(\lambda+1)C_f & (\frac{l_r}{l_f}-\lambda)C_r & -\lambda\frac{m}{2} \end{bmatrix} \begin{bmatrix} \delta_{f,ss} \\ x_{1,ss} \\ x_{2,ss} \\ v_x r_{ss} \end{bmatrix} = 0 \tag{30}$$

where the subscript ss indicates a constant quantity. In theory, regression methods can be applied to (30) to estimate C_f, C_r, $\frac{l_r}{l_f}$, and m if at least four independent sets of measurements of x_1, x_2, and $v_x r$ that correspond to the same front wheel angle are supplied. Obtaining such measurements are unfortunately not possible since there is no way to know for certain that two different sets of measurements of x_1, x_2, and $v_x r$ belong to the same front wheel angle.

On a final note, the above result also implies that the well-known steady-state cornering equation

$$\delta_f = L\frac{r}{v_x} + \frac{K_{us}}{g} v_x r, \tag{31}$$

which can be derived from the linear single-track model cannot be used fully to estimate the front wheel angle. The reason for this is that the understeer gradient, K_{us}, cannot be estimated. To demonstrate the relevance of the term that includes the understeer gradient Fig. 14 shows the measured SWA during a manoeuvre and also the quantity $L\frac{r}{v_x}$ computed from sensor measurements and thereafter converted to SWA.

The understeer gradient can be expected to be positive by design of the vehicle since it gives stable handling properties and can range up to several degrees per m/s^2 lateral acceleration in more heavily understeer trucks and tractor-trailer combinations [13]. In a truck with an understeer gradient of $5\,^\circ/m/s^2$ and a gear ratio of 1:20 between front wheel angle and SWA, there would be a $100\,^\circ$ error per m/s^2 lateral acceleration if the SWA is estimated by only using the term $L\frac{r}{v_x}$ of (31). On the other hand, the vehicle that was used to produce the SWA estimates in Fig. 14 had an understeer gradient of about $0.4\,^\circ/m/s^2$, giving rise to about 15-20 $^\circ$ estimation error when cornering with a maximum lateral acceleration around 2 m/s^2.

4.3 Summary, conclusions, and further work

Considering the large amount of vehicle configurations that Scania CV delivers, an estimation principle will be the more useful the less specific it is to a certain vehicle. For this reason two basic approaches to estimate the SWA has been investigated, and it is found that both of these at best can estimate an angle that corresponds to the Ackermann steering angle. This means that the estimates obtained are unbiased only when the vehicle is cornering at low lateral acceleration.

The presented estimation results are produced directly by using measurement data as input to the respective models. More advanced estimation schemes such as the Kalman filter can be applied to produce a less noisy estimate of the SWA but will not help to

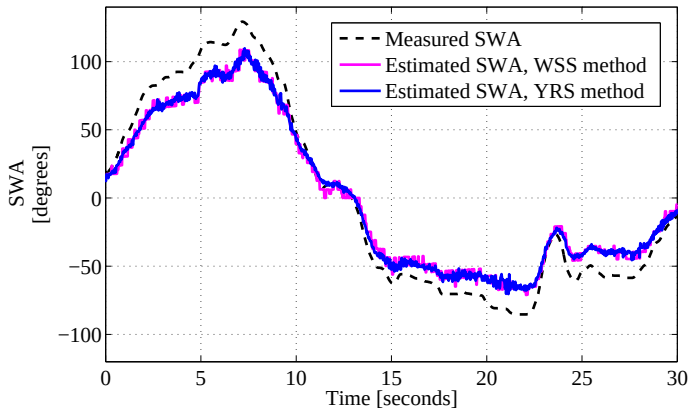

Figure 14: Estimated SWA during the same manoeuvre as in Fig. 11. The SWA estimate marked WSS is computed with the method covered in section 4.1 while the estimate labeled YRS is computed based on measurements from the yaw rate sensor.

overcome the fact that the underlying models are biased, likely on the order of tens of degrees, when the vehicle corners at high speed. For the purpose of estimating the SWA at all speeds, the larger improvement in accuracy will therefore come from developing less biased models.

To be able to estimate the SWA more accurately when the vehicle is cornering under significant lateral acceleration, further investigation may include to quantify how the range of the understeer gradient depends on the vehicle's configuration and the mass of the payload and how it is distributed. Another way forward may be to investigate how the slip angles of the front and rear wheels correlate with the different quantities measured by the sensors, especially the rotational speeds of the front wheels.

5 Offset estimation

The SWA offset can be defined as the SWA needed to drive perfectly straight under circumstances when the vehicle is not pulled sideways by forces/moments from braking, accelerating, horizontal road slope, and/or aerodynamic phenomena. In the case where there is a significant backlash in the steering system, the definition of SWA offset used here will be the midpoint of the backlash.

The presented algorithm estimates the SWA offset for the vehicle's *current* wheel alignment. This means that if the algorithm's most recent output is significantly different from its previous output the underlying reason could be due to change in wheel alignment, tire/suspension properties and/or the mounting of the SAS. Also, the horizontal slope of the road is compensated for but aerodynamic effects are neglected. Therefore, if the vehicle is driven in strong cross-wind for a longer time, the SWA offset estimated during this time may be slightly off.

The signals used in the function are steering wheel angle, yaw rate, vehicle speed, and lateral acceleration, and the method of estimation is built on a least mean squares approach combined with a simple vehicle model for steady-state cornering.

5.1 Description of the estimation algorithm

The SWA offset estimation algorithm works by the fundamental principle that it continuously monitors key parameters related to the vehicle's motion, and when these indicate certain driving conditions the estimation of SWA offset is activated. This approach allows for use of relatively simple mathematical models and a low computational complexity of the algorithm.

The conditions when the algorithm activates the estimation of SWA offset can be summarised as when the vehicle is driven

1. with nearly constant longitudinal speed,
2. with longitudinal speed exceeding 10 m/s,
3. constantly nearly straight-ahead, and
4. when the road bank angle is that of common roads.

Condition 1 is included due to the fact that the vehicle may pull to the side when braking or accelerating, phenomena often referred to as brake pull and torque steer,

Symbol	Description	Type
r	Yaw rate	Measured
v_x	Longitudinal speed	Measured
δ	Steering wheel angle	Measured
a_y	Lateral acceleration	Measured
L	Vehicle wheelbase	Supplied parameter
i_{gear}	Overall steering gear ratio	Supplied parameter
$\hat{a}_g$	Est. component of the gravitational acc.	Estimated
$\hat{\dot{v}}_x$	Longitudinal acceleration	Estimated
$\hat{R}^{-1}$	Inverse turn radius	Estimated
$\hat{\delta}$	Est. SWA	Estimated
$\hat{\delta}_o$	Est. SWA offset	Estimated

Table 3: List of signals, parameters and estimated quantities used in the algorithm.

respectively.

Condition 2 is mainly used for the cornering (10) to be valid. An additional benefit of imposing condition 2 is that no estimation is carried out at low speeds, e.g. parking speeds, because torsion of the steering system generally is greater at those speeds, which in turn would increase uncertainty of the estimated SWA offset or require more thorough modelling of the steering system.

Condition 3 is imposed because it is beneficial to estimate the SWA offset when the torque in the steering system frequently changes sign or is near zero. This has to do with backlash in the steering system and is explained further in section 5.3. Also, the combination of conditions 1, 2, and 3 resembles steady-state cornering and therefore makes it possible to use (10).

Finally, the purpose of using condition 4 is to avoid estimation during times when the vehicle is pulled sideways due to a large banking of the road.

Fig. 15 illustrates a flowchart of the algorithm and the symbols used throughout this chapter are listed in Tab. 3.

5.1.1 Signal pre-processing

To begin with, all signals received via the CAN except the SWA signal are low-pass filtered with identical 2^{nd} order infinite impulse response filters. These have a cut-off

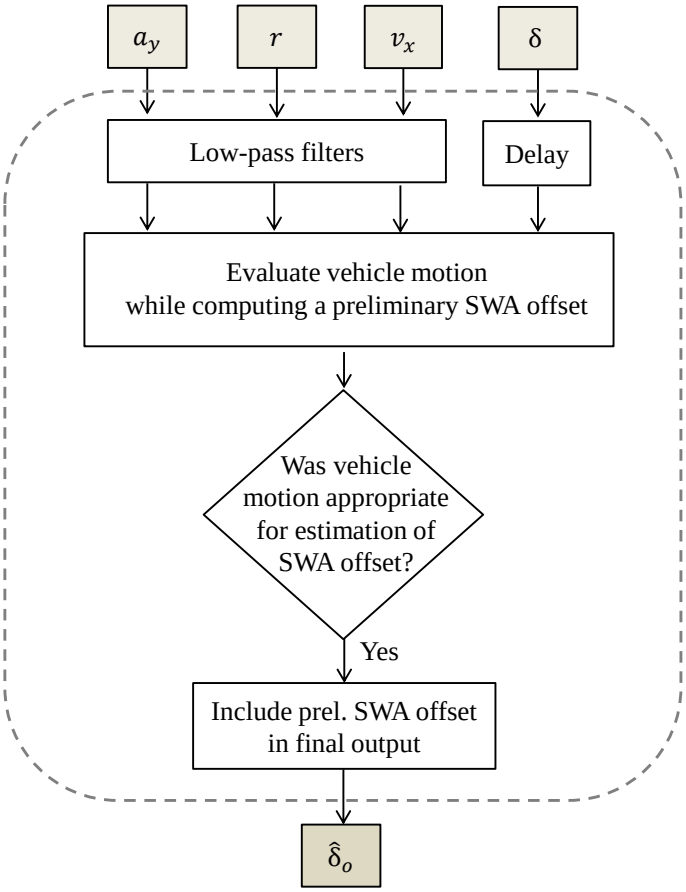

Figure 15: Overall structure of the SWA offset estimation algorithm. Symbols are defined as listed in Tab. 3.

frequency of 3 Hz and are designed to have a maximally flat frequency response in the pass band. This filtering is needed for the function that decides if the estimation should be active or not.

To keep the SWA signal synchronised with the filtered signals it is delayed with the corresponding group delay around 0-2 Hz introduced by the filters.

5.1.2 Evaluation of the vehicle's motion

To evaluate the vehicle's motion three complementary quantities are estimated. The first being the inverse turn radius is estimated as

$$\hat{R}^{-1} = \frac{r}{v_x}. \tag{32}$$

The inverse is used to avoid potential numerical problems when the vehicle is driven straight-ahead.

The second estimated complementary quantity is the longitudinal acceleration, which is estimated directly from the longitudinal speed signal with a down-sampled version of a smoothing differentiator. This works well because the longitudinal speed varies sufficiently slowly in heavy trucks. Computationally costly operations related to real-time differentiation are also significantly reduced.

Finally, the third estimated quantity is the lateral acceleration resulting from road bank angle and is estimated as

$$\hat{a}_g = a_y - rv_x. \tag{33}$$

An underlying assumption for (33) to be valid is that $\dot{v}_y = 0$.

The conditions

$$\begin{cases} \dot{r} = 0 \\ \dot{v}_x = 0 \\ \dot{v}_y = 0 \end{cases}$$

correspond to a state of steady-state cornering [14], and in the algorithm this state is approximated as

$$\begin{cases} max\{\ |\hat{R}^{-1}[t]|\ \}_t < R_{max}^{-1}, & t = t_0, ..., t_1 \\ |\hat{\dot{v}}_x| < \dot{v}_{x,max} \end{cases} \tag{34}$$

meaning that, again, the assumtion $\dot{v}_y \approx 0$ is made.

The first condition in (34) implies that the turn radius must be sufficiently large during a time span $t_1 - t_0$. In other words the vehicle must be driven nearly straight with mean yaw acceleration being roughly zero. If this constraint on yaw acceleration is not included, unwanted SWA measurements during transient motions will enter the SWA offset estimation. The motivation for approximating $\dot{r} \approx 0$ with this approach is because the yaw rate signal by nature is quickly varying and noisy. Also, even with a highly

accurate estimate of the yaw acceleration, it is difficult to use it alone to distinguish between transient and steady-state vehicle motion.

The road bank angle is controlled to be not too high by imposing the limit

$$max\{\ \left|\hat{a}_g[t]\right|\ \}_t < a_{y,max}, \qquad t = t_0, ..., t_1. \tag{35}$$

The operations described above introduce a time-delay of t_1, and during that time temporary estimates of the SWA offset and the understeer gradient are computed.

The values $\dot{v}_{x,max}$, R_{max}^{-1}, $a_{y,max}$, and t_1 are preset and are presented and discussed further in section 5.4.

5.1.3 Computation of SWA offset

The SWA offset is computed with a recursive least mean squares method as

$$\hat{\delta}_o[k] = \hat{\delta}_o[k-1] + \frac{\delta_m[k] - \hat{\delta}[k] - \hat{\delta}_o[k-1]}{k}, \qquad k = 1, 2, ..., N \tag{36}$$

where N is the total number of included SWA measurements and

$$\hat{\delta}[k] = i_{gear}\left(L\frac{r[k]}{v_x[k]} + \frac{\hat{K}_{us}[k]}{g}\big(r[k]v_x[k] + \hat{a}_g[k]\big)\right), \tag{37}$$

which is the steady-state cornering equation described in section 2.4.1.

The term $\hat{K}_{us}$ in (37) represents the vehicle's understeer gradient and is estimated separately from the SWA offset. This is because the SWA offset is estimated when the vehicle is driven nearly straight-ahead, which are circumstances where backlash-like effects of the measured SWA have high magnitude relative to the SWA estimated with the model in (37). This, in turn, makes estimation of K_{us} by linear regression unsuitable.

Another criteria regarding the estimation of K_{us} is due to the large variety in axle configuration in Scania CV's product line. A vehicle's understeer characteristics is largely determined by the number of axles, the distances between those, and the number of tires on each axle. Asymmetries in the suspension and steering system may also lead a vehicle having different understeer characteristics depending on the direction of turn. As these effects usually have the largest impact at higher lateral accelerations, K_{us} is estimated at time instants where the lateral acceleration is below 1.5 m/s^2. This value was found by examining a number of handling diagrams for vehicles with different axle configurations.

Also, the estimation of K_{us} needs fairly unbiased measurements of SWA. For this reason $\hat{K}_{us}$ is at first set to zero and when the SWA offset estimate is accurate enough

the estimation of K_{us} is carried out with the same type of linear regression as (36) according to the relation

$$\hat{K}_{us} = \frac{g}{rv_x}\left(\frac{\delta_m - \hat{\delta}_o}{i_{gear}} - L\frac{r}{v_x}\right). \tag{38}$$

5.2 Statistical foundation of the estimation principle

Equation (36) is the result of modelling the measured SWA as

$$\delta[k] = \delta_o[k] + \delta_{true}[k], \qquad k = 1, 2, ..., N \tag{39}$$

where δ_{true} is the unbiased SWA. By substituting δ_{true} with the approximation

$$\delta_{true}[k] = \hat{\delta}[k] + \epsilon[k], \qquad k = 1, 2, ..., N \tag{40}$$

where ϵ is the modelling error, (39) becomes

$$\delta[k] = \delta_o[k] + \hat{\delta}[k] + \epsilon[k], \qquad k = 1, 2, ..., N \tag{41}$$

and from this equation the ordinary least squares (OLS) estimate of δ_o becomes

$$\hat{\delta}_o = \frac{1}{N}\sum_{k=1}^{N}\big(\delta[k] - \hat{\delta}[k]\big), \tag{42}$$

which can be re-formulated into the recursive (36).

By the Gauss-Markov theorem, the OLS estimate is the linear unbiased estimator with the lowest possible variance if the error term ϵ in (41) has zero mean, zero autocovariance, and constant variance.

Due to a number of reasons it is clear that (42) is statistically sub-optimal for the estimation of SWA offset. One reason is due to the nonlinearity, e.g. backlash, included in a function describing the SWA, and another is that a sequence of measured SWA values will not have zero autocovariance as the measured SWA greatly depends on the curvature of the road. If, for example, the vehicle undergoes a constant-radius turn for 10 seconds the measured SWA values will be highly correlated for a 10 second period. Therefore, as an approximation of the SWA will not be perfect the error term in (41) will have non-zero autocovariance.

However, the fact that (42) can be reformulated into the recursive form of (36) is very favorable from a computational point of view. This combined with satisfactory accuracy during in-field tests is the reason for choosing this estimator.

The variance of the estimator is

$$var(\hat{\delta}_o) = \frac{1}{N^2}\sum_{k=1}^{N} var\big(\delta[k] - \hat{\delta}[k]\big). \tag{43}$$

In simulations in was found that the quantity $\delta[k] - \hat{\delta}[k]$ rarely exceeds $10\,^\circ$, leading to the conclusion that the variance of the estimator in (36) is very low for large N. As the sampling rate of the used signals in the algorithm usually is around 50-100 Hz, N will grow large in a short period of time.

An expression of the bias of the estimator can be derived as

$$\begin{aligned}\hat{\delta}_{o,error} \triangleq E\big[\delta_o - \hat{\delta}_o\big] &= \delta_o - \frac{1}{N}\sum_{k=1}^{N} E\Big[\delta[k] - \hat{\delta}[k]\Big] \\ &= \delta_o - \frac{1}{N}\sum_{k=1}^{N} E\Big[\delta_o[k] + \delta_{true}[k] - \hat{\delta}[k]\Big] \\ &= \frac{1}{N}\sum_{k=1}^{N} E\Big[\hat{\delta}[k] - \delta_{true}[k]\Big],\end{aligned} \tag{44}$$

and as can be seen, the bias depends on the difference between the estimated SWA and the theoretically unbiased SWA.

From here, there are different ways to take the analysis further. One way is to assume that the steady-state description 10 can perfectly describe the SWA. By doing so, (44) can be formulated in terms of the quantities used in the estimation (r, v_x, and $a_{y,g}$) in their measured and theoretically unbiased forms.

By modelling the errors in yaw rate and lateral acceleration as offsets and the error in longitudinal speed as a scaling error caused by an error in wheel radii according to

$$\begin{cases} r = r_o + \tilde{r} \\ a_g = a_{g,o} + \tilde{a}_g \\ v_x = \tilde{v}_x(1+\lambda) \end{cases} \tag{45}$$

and the unbiased SWA as

$$\delta_{true} = i_{gear}\left(L\frac{\tilde{r}}{\tilde{v}_x} + \frac{\hat{K}_{us}}{g}\big(\tilde{r}\tilde{v}_x + \tilde{a}_g\big)\right) \tag{46}$$

we get that

$$\hat{\delta}_{o,error} = i_{gear}\,E\left[\,L\frac{r_o - \lambda\tilde{r}}{\tilde{v}_x(1+\lambda)} + \frac{\hat{K}_{us}}{g}\Big(r_o\tilde{v}_x(1+\lambda) + \lambda\tilde{r}\tilde{v}_x + a_{g,o}\Big)\right]. \tag{47}$$

When the vehicle is driven nearly straight-ahead for longer periods of time the quantity $E[\lambda\tilde{r}]$ will be negligibly small compared to the other terms and (47) can then be simplified into

$$\hat{\delta}_{o,error} = i_{gear}\left(\frac{1}{E[\tilde{v}_x]}\frac{L}{1+\lambda} + E[\tilde{v}_x]\frac{\hat{K}_{us}(1+\lambda)}{g}\right)r_o + \frac{i_{gear}\hat{K}_{us}}{g}a_{g,o}. \tag{48}$$

Equation 48 shows how the bias of the SWA offset estimator depends on errors in the sensors used in the estimation, and the overall impact of these errors are studied in the following chapter.

5.3 Theoretical performance

As mentioned in section 2.5 the raw gyroscope output has a bias that may be as large as $3\,^\circ/s$ and the raw accelerometer output might be biased by almost 1 m/s^2.

Fig. 16 shows how such biases impact the SWA offset estimate based on (48). For comparison, typical values of wheelbase and understeer gradient are chosen to represent a heavily understeered tractor-semitrailer combination and also a distribution truck with a much lower understeer gradient. The used parameters for these vehicles are realistic but does not correspond to any specific, existing vehicles.

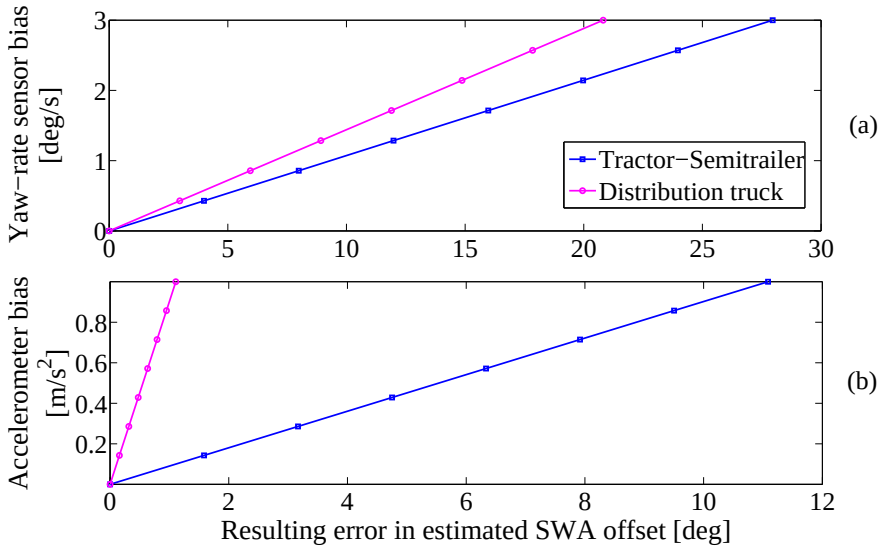

Figure 16: The effect of YRS and accelerometer bias approximated with (48) with parameter values $E[v_x] = 15$ m/s, $\lambda = 5\%$, and $i_{gear} = 19$.

5.3.1 Errors related to the yaw rate sensor

Fig. 16a shows the importance of compensating the YRS bias. To test the performance of a method to estimate the YRS bias error, a sensor fusion approach presented by Gustafsson et al. [15] was simulated. This approach uses a Kalman filter with yaw rate and wheel rotational speeds as inputs and one of the filter's state variables is the YRS bias. Fig. 17 shows the results of the implementation. A linear bias drift of $0.5\,^{\circ}/s/min$ was added to test the performance. As can be seen at approximately 6 minutes the filter is not able to track the changing offset, which may be the result of the input signals being nearly constant (the vehicle was driven straight-ahead) and also that the used wheel speed data were quantified to low resolution. An easy solution to this problem would for example be to use a cumulative sum (CUSUM) test to identify if the YRS bias is highly time-varying, and if so the SWA offset estimation can be deactivated.

However, the important conclusion to be made is that easily implementable methods are applicable to compensate YRS bias well enough to make the SWA offset estimation accurate. With a maximum $0.2\,^{\circ}/s$ YRS bias the SWA offset estimation error is less than approximately $1.5\,^{\circ}$.

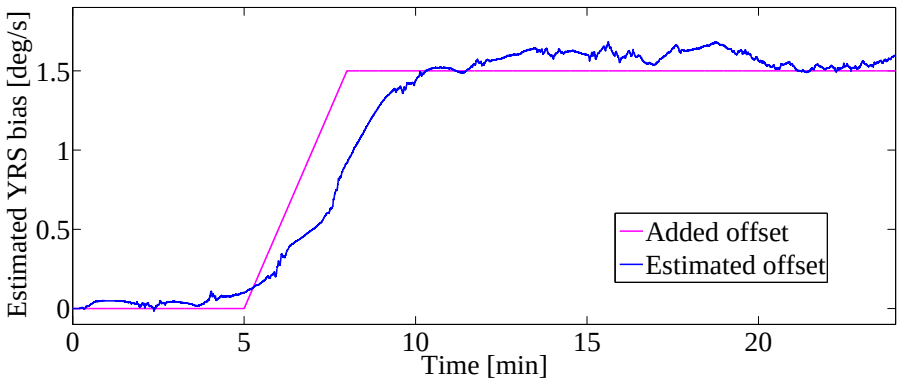

Figure 17: Performance evaluation of a method to estimate YRS bias.

5.3.2 Errors related to the accelerometer

As can be seen in Fig. 16b, an accelerometer bias affects the SWA offset estimate to a larger extent in the heavily understeer vehicle.

The accelerometer offset can also be viewed as a road bank angle. As explained in section 2.5 common road bank angles generate sensor readings of about 0.2 m/s^2 and in

extreme cases closer to 1 m/s^2. Therefore, for purposes where up to a $10\,^\circ/s$ SWA offset estimation error is acceptable or if the specific vehicle configuration has a low understeer gradient, there is no need to use the accelerometer signal in the algorithm. However, it is fairly safe to assume that this error will be significantly lower if the SWA offset estimation is carried out over a long period of time, e.g. during hours of driving, due to variation in road bank angle.

The topic of estimating the accelerometer bias is left out of the scope of this thesis but the implications are discussed further in section 5.5.

5.3.3 Errors related to backlash in the steering system

The estimation principle is based on a linear model, and because there are nonlinearities in a function that best describes the SWA it is necessary to investigate how these will affect the estimate. Assuming the backlash in the steering system is the dominant nonlinearity under the driving conditions when the offset estimation is active, the introduced error will be additive to (48). More specifically, if the estimate is computed from N samples this error will be

$$\epsilon_{fp} = \frac{1}{N}\sum_{k=1}^{N} B[k], \tag{49}$$

where $B[k]$ represents the position of the backlash at time sample k. A maintenance standard of at most $15\,^\circ$ backlash corresponds to

$$-7.5\,^\circ \leq B[k] \leq 7.5\,^\circ \tag{50}$$

and hence the error is bound as

$$-7.5\,^\circ \leq \epsilon_B \leq 7.5\,^\circ. \tag{51}$$

An intuitive way to analyse this error is in terms of histograms of $B[k]$ such as the hypothetical ones illustrated in Fig. 18. The histogram on the left of Fig. 18 shows a symmetrical distribution whereas the right one shows a distribution that is skewed to towards positive angles. Applying (49) to these distributions, in other words taking the arithmetic mean, yields an error that is zero for the symmetrical distribution and non-zero and positive for the skewed distribution.

The fact that a driver constantly adjusts the vehicle's heading may seem as a useful feature that reduces this error caused by the backlash. If the steering wheel is periodically turned back and forth such that the backlash moves from its one end to its other, the

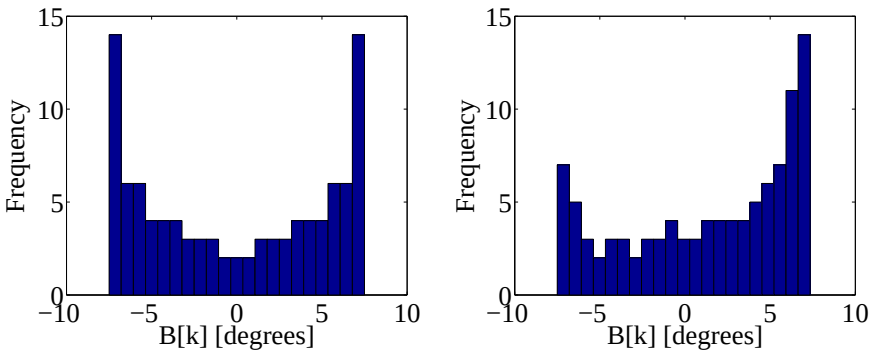

Figure 18: Two possible distributions of the position of the backlash $B[k]$

distribution of $B[k]$ will be symmetrical and therefore causes no error in the SWA offset estimation. However, such a periodic motion is no guarantee that the backlash moves over its full span as this requires the torque applied at the steering wheel to change sign. During cornering, for example, the self-aligning moment of the tires makes it possible to change the heading of the vehicle by simply increasing or decreasing the torque applied at the steering wheel. The same may also be possible when driving in strong side wind or on roads with high enough bank angle.

A certain case that is important to consider is if the vehicle constantly pulls to one side, e.g. due to incorrect wheel alignment. In this case $B[k]$ may be distributed similarly to the right plot of Fig. 18 but being even more skewed. In the worst case, the torque at the steering wheel does never change sign, causing a 7.5° error to the estimated offset.

In contrast, a vehicle that handles properly is expected to sometimes generate a distribution of $B[k]$ such as the right plot of Fig. 18, while at other times generate mirrored versions of this distribution. This is under the assumtion that the vehicle is sometimes yawed mostly to the left and other times mostly to the right. In a vehicle that has a 15 ° backlash, this would correspond to the error in estimated SWA being in the range 0 ° to 7.5 ° when yawing to the left and when yawing to the right the error would be in the range -7.5 ° to 0 °.

5.4 Results

The recorded CAN signals from the 30 minute drive were imported to MATLAB Simulink and tested with the SWA offset estimation algorithm described in section 5.1.

During the test drive, the vehicle was driven mostly back and forth along the straight,

1.5 km long, diagonal path seen in Fig. 8. As a result of repeatedly driving in a loop on the same path, the mean SWA occasionally coincided with the 2.04 ° offset estimated in section 3. For this reason the algorithm performance is evaluated when driving once over this straight path.

The simulation results are presented in Fig. 19 where each line correspond to a single drive across the track, and the round markers represent the final value of the estimated SWA offset. It should also be noted that the algorithm was re-initialised at the start of each estimation. The parameters in the algorithm was set as presented in Tab. 4. It

R_{max}^{-1}	$(800\ m)^{-1}$
$\dot{v}_{x,max}$	$0.3\ m/s^2$
$a_{y,max}$	$0.3\ m/s^2$
t_1	$2\ s$

Table 4: Threshold parameters used in the simulation presented in Fig. 19.

is seen in Fig. 19 that the estimations were carried out for different amounts of time. This is due to the algorithm's function that activates estimation according to the criteria listed in section 5.1.

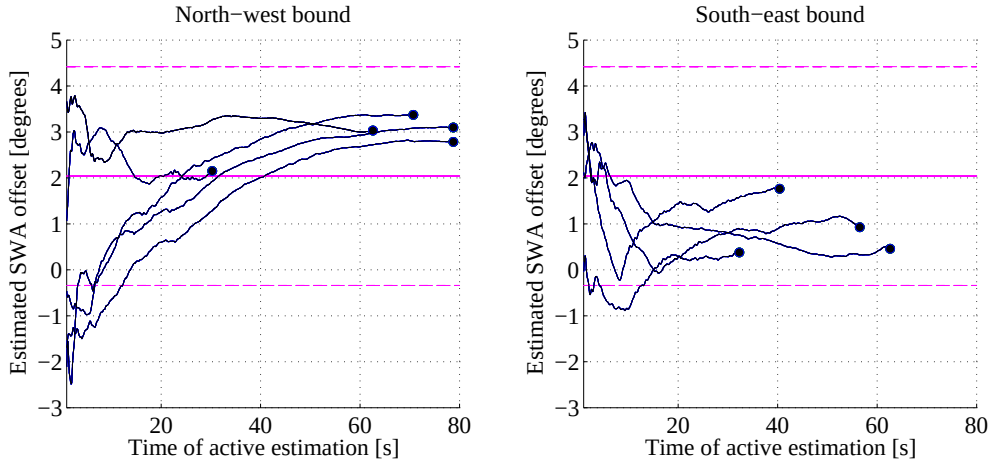

Figure 19: Estimated SWA offset during different runs driving in the north-west and south-east direction on the test track. The solid horizontal lines mark the vehicle's measured mean SWA offset and the dashed horizontal lines represent the corresponding 95% confidence interval.

In Fig. 19 it is also seen that the different SWA offset estimates are distributed

within the 95% confidence interval. The estimates produced when driving in the north-west direction generally lie above the mean, and the estimates produced when driving south-east lie below the mean.

5.5 Discussion

5.5.1 Possible further processing of the SWA estimate

Due to the backlash in the steering system the algorithm output should theoretically vary over at least the width of the backlash. This may be the behavior seen in Fig. 19 where the final estimates are distributed between zero and four degrees.

The backlash could also explain why the estimates differ depending on if the vehicle is driven in the north-west or the south-east direction. The results in Fig. 19 are consistent with the slight curvature of the track in the sense that driving in the north-west direction requires the average SWA to be positive and in the south-east direction a negative average SWA is required. This, in turn, leads to corresponding errors caused by the backlash to be positive and negative, respectively, as seen in Fig. 19.

If simply running the estimation during several traveled kilometers it is possible that the estimate will be biased due to the vehicle yawing more in one direction than the other as in Fig. 19. A situation where this is likely to happen is when the vehicle is driven on a typical long, arc shaped road that bypasses a larger city.

To further increase the accuracy of the estimated SWA offset the midpoint of the backlash has to be estimated. A simple, ad-hoc way to do so is to perform the estimation multiple times and sort the obtained values into two bins that correspond to the average lateral acceleration being positive or negative during the estimation. In other words, the estimated SWA offsets would be labelled as being produced while the vehicle yawed to the left or to the right. The enhanced SWA offset estimate would then be obtained by computing the mean of each bin and finally computing the mean of those two values. Based on Fig. 19 and the fact that the mean velocity of the vehicle was about 15 m/s, a sufficient distance over which each of these estimations should be active is at least 300 m, corresponding to about 20 seconds of active estimation in Fig. 19.

Another more efficient approach is to modify the algorithm to use an adaptive filter such as the Recursive Least Squares (RLS) filter instead of the OLS filter that the presented algorithm uses. The estimated SWA offset will then be based mostly on the most recent measurements. By finding somewhat stationary values in the estimated SWA

offset and sorting them into bins as previously mentioned an estimate of the midpoint of the backlash may be obtained more quickly.

The above approaches increase the likelihood that the estimate will be closer to the midpoint of the backlash but does not guarantee this. In a vehicle that constantly pulls to one side this approach will not work because the distribution of the position of the backlash will be heavily skewed to one side. For more definitive assessment of the backlash, information about the torque in the steering system has to be supplied, e.g. by using a steering torque sensor.

5.5.2 Efficacy of the motion filter

The function that activates the estimation based on the vehicle's motion has not been put to test with a vehicle that develops torque steer and/or brake pull, and neither has this function been tested on roads with bank angle that is higher than normal. Therefore, the parameters listed in Fig. 4 should be considered to be more safe than optimal. These parameters were chosen based on the data that were gathered from the test vehicle by considering how fast the estimation achieves good accuracy, i.e. how often it activates, and also the variance of the estimate. For a more general set of parameters, the algorithm should be tested on a wider range of vehicles.

5.5.3 The accelerometer signal

The accelerometer signal is included for completeness of the algorithm but may in practice be of less benefit. This is because the road bank angle of common roads is expected to introduce negligible estimation error in nearly neutrally steer trucks and an estimation error of about $2\,^\circ$ in heavily understeer ones as shown in Fig. 16b. Considering the worst-case performance of the typical automotive-grade MEMS accelerometer, 1 m/s^2 bias and possibly changing at 0.3 $m/s^2/min$, it is realised that including this sensor might actually worsen the performance. For this reason it is recommended that the bias properties of the actual, post-processed accelerometer signal that is broadcast on the CAN is examined before performing an implementation of the algorithm that uses the accelerometer signal.

5.5.4 Using other sensors for the estimation

The algorithm described in section 5.1 can straightforwardly be modified to operate using only wheel speed sensors and the SAS. To do so, the lateral acceleration is simply excluded and by using the wheel speed sensor signals the following by substitutions are to be made:

- $v_x = \frac{v_{rl}+v_{rr}}{2}$
- $\hat{R}^{-1} = \frac{v_{fl}+v_{fr}}{2} \frac{2}{L_{tw}\cos(\frac{\delta-\delta_o}{i_{gear}})} \frac{v_{fr}/v_{fl}-1}{v_{fr}/v_{fl}+1}$
- $\hat{\delta} = i_{gear}\frac{1}{2}\sin(\frac{4L}{L_{tw}}\frac{v_{fr}-v_{fl}}{v_{fr}+v_{fl}})$.

Subscripts rl, rr, fl, and fr indicate wheel speeds of the rear left, rear right, front left, and front right wheel respectively, and L_{tw} is the rear axle track width. The origin of the equations are explained in section 2.2.

Further, it should be noted that this way of detection requires estimation of tire radii. This is possible using only wheel speed sensors but requires some time for convergence of the tire radii estimates.

5.6 Summary, conclusions, and further work

The developed algorithm is an ordinary least squares estimator combined with a function that activates the estimation when the vehicle is traveling with suitable speed, turn radius, and acceleration. In the well serviced vehicle on which the algorithm was tested the estimation error was less than $2\,^\circ$, and with further improvements to the algorithm it is believed that this error can be reduced to under $1\,^\circ$. In terms of computational requirements the algorithm is considered to be of low complexity.

It is argued that a backlash in the steering system is possibly the largest source of error that, assuming a maintenance standard of $15\,^\circ$, may contribute with as much as $7.5\,^\circ$ estimation error. Vehicles that spontaneously pull to one side can be expected to accumulate this kind of error.

Further work may include to investigate the bias properties of the accelerometer and YRS to finally test and implement the algorithm, and further improvements will be to research better parameters for the function that activates the estimation and also how to compensate for backlash in the steering system.

References

[1] S. Bennett, A. Norman, *'Heavy Duty Truck Systems'*. Clifton Park, New York, USA: Delmar Cengage Learning, 2011.

[2] G. Gim, 'Subjective and Objective Evaluations of Car Handling and Ride', *Road and Off-road Vehicle System Dynamics Handbook*. CRC Press, 2014.

[3] T. D. Gillespie, *Fundamentals of Vehicle Dynamics*. Warrendale, Pennsylvania, USA: SAE International, 1992.

[4] J. Aurell, 'Dynamics of Heavy Commercial Vehicles and Buses', *Road and Off-road Vehicle System Dynamics Handbook*. CRC Press, 2014.

[5] J. Y. Wong, *Theory of Ground Vehicles*. New York, USA: Wiley, 2001.

[6] G. Rill, *Road Vehicle Dynamics: Fundamentals and Modeling*. CRC Press, 2012.

[7] H. Pacejka, *Tire and Vehicle Dynamics*. 3rd Edition, Elsevier, 2012.

[8] C. B. Winkler, "Simplified Analysis of the Steady-State Turning of Complex Vehicles," *Vehicle System Dynamics*, vol. 29, no. 3, pp. 141-180, 1998.

[9] Gulmammadov, F., "Analysis, modeling and compensation of bias drift in MEMS inertial sensors," in *Recent Advances in Space Technologies, 2009. RAST '09. 4th International Conference on*, pp.591-596, June 2009.

[10] L. E. Hall, R.D. Powers, D.S. Turner, W. Brilon and J. W. Hal, "Overview of Cross Section Design Elements," in *International Symposium on Highway Geometric Design Practices, Boston, Massachusetts, August 30 - September 1, 1995. Conference Proceedings*, Jan 1998.

[11] Klier W., Reim A., Stapel D., "Robust Estimation of Vehicle Sideslip Angle - An Approach w/o Vehicle and Tire Models," *SAE Technical Paper 2008-01-0582*, 2008.

[12] Bevly, David M., and Cobb, Stewart, *GNSS for Vehicle Control* . Norwood, USA: Artech House Books, 2010.

[13] ARRB Transport Research, "Assessment of Truck/Trailer Dynamics," *Technical Working Paper*, No. 31, Dec 1997.

[14] M. Abe and W. Manning, *Vehicle handling dynamics: theory and application*. Amsterdam Boston: Butterworth-Heinemann/Elsevier, 2009.

[15] Gustafsson, F., Ahlqvist, S., Forssell, U., and Persson, N., "Sensor Fusion for Accurate Computation of Yaw Rate and Absolute Velocity," *SAE Technical Paper 2001-01-1064*, 2001.